Cotton Fabric Incorporated with β-Cyclodextrin/Ketoconazole/Ag-NPs Generating Outstanding Antifungal and Antibacterial Performances

Nafiseh Hedayati
Amirkabir University of Technology
Majid Montazer (tex5mm@aut.ac.ir)
Amirkabir University of Technology https://orcid.org/0000-0002-1983-6735
Mahnaz Mahmoudirad
Shahid Beheshti University of Medical Sciences School of Nursing and Midwifery
Tayebeh Toliyat
Tehran University of Medical Sciences

Research Article

Keywords: β-cyclodextrin/Ketoconazole/Ag nanocomposites, Drug delivery, Antimicrobial properties, Cotton fabric

Posted Date: March 2nd, 2021

DOI: https://doi.org/10.21203/rs.3.rs-255381/v1

Abstract

The influence of Ketoconazole and β-CD/Ketoconazole was previously reported on cotton fabric as fungal skincare; however, the impact of nanosilver on the antifungal and antibacterial properties of the same products is unknown. Here, silver NPs were synthesized on β-CD/KZ composites and then attached to the cotton using a cross-linking agent. The nanocomposites and treated fabrics were analyzed by UV-vis, dynamic light scattering (DLS), zeta-potential and FE-SEM. The drug delivery and cytotoxicity of the products were also studied. The nanocomposites antimicrobial efficiency was examined on *Candida albicans* and *Aspergillus niger* as fungi and *E. coli* & *S. aureus* as bacteria. The synthesis of Ag-NPs on the β-CD/KZ amplifies both antifungal and antibacterial efficiencies. This also extends the drug regular release time for medical and drug delivery purposes. Having tremendous antimicrobial activities without cytotoxicity effects and regular release time of drug with excellent washing durability of treated samples make it suitable for medical applications likewise wound dressings and sportswear designed for sensitive skin.

Introduction

Human skin covers the whole body that in contact with the environment generates most injuries such as wounds, burns and skin fungi (Benita 2006; Farokhi et al. 2018; Kim et al. 2019; Wu et al. 2018). This immense surface is easily accessible for drug delivery as a painless and non-invasive method. Topical drug delivery has advantages such as high drug concentration on the skin, lower side-effects, ease of transfer, more sustainability and water solubility (Benita 2006; Farokhi et al. 2018; Kim et al. 2019; Lee et al. 2017). Therefore, diverse chemical and physical technologies were adapted to improve drug delivery via the skin. On this base, nanoparticles were used to extend half-life, decrease drug dosage and improve drug properties (Farokhi et al. 2018; Kim et al. 2019; Lee et al. 2017; Veerakumar et al. 2020; Wang et al. 2015). Nevertheless, a dressing substrate with drug release properties such as cotton treated with cyclodextrin (CD) can be useful for this purpose (Ning et al. 2020; Pinho et al. 2014; Radu et al. 2016; Sharaf and El-Naggar 2019; Yao et al. 2019). Because, β-cyclodextrin (β–CD) with the hydrophobic cavity and hydrophilic surface can control the release of aromatic compounds (Abarca et al. 2016).

It is well-known that Ketoconazole (KZ), as an antifungal and water-insoluble drug with high molecular weight, is often used topically to treat superficial fungal infection (Che et al. 2015), especially *Candida albicans* (Kaur & Kakkar 2010). The entrapped KZ in β–CD showed antifungal properties without antibacterial effects (Kaushik et al. 2017; Rameshkumar et al. 2003). However, introducing nanoparticles to the antimicrobial drugs has a significant synergistic effect, entering into the cell wall carrying more antibiotic into the cell, causing cell death (Durán et al. 2016; Jiang et al. 2019; Rana et al. 2016; Sedighi et al. 2014). Further, capping Ag-NPs with β-CD improved their efficacy and cytotoxicity (Gupta et al. 2020). Nevertheless, the combination of KZ/Ag-NPs showed the most synergistic effects in comparing with the common antifungal drugs such as Nystatin, Fluconazole and Clotrimazole (Falahati et al. 2014; Jiang et al. 2019; Rana et al. 2016; Sedighi et al. 2014).

In our previous study, KZ and β-CD/KZ were loaded on the cotton fabric via padding by immersing the fabric in the prepared solution, squeezed and finally dried at 80 ˚C. This was also done through exhaustion by immersing the fabric in the prepared solution heated for 1 h at 80 ˚C along with stirring and final drying at 80 ˚C. We investigated and reported the drug release, antimicrobial activities and cytotoxicity of the products (Hedayati et al. 2020). The KZ release rate was prolonged, especially in the exhaustion method compared with the other drugs release from the samples reported by others. Also, β-CD/KZ showed antifungal properties with no inhibition zone against bacteria (Hedayati et al. 2020). Here, Ag-NPs were synthesized on β-CD/KZ to improve the antimicrobial properties and moderate the release rate. KZ was entrapped in β-CD, then Ag-NPs synthesized on the β-CD/KZ composites successively loaded on the cotton fabric with two exhaustion and padding methods.

The sample with the most antimicrobial activities and slow/regular drug release, besides the highest washing durability, breathability and moisture absorption, was selected as the best sample. This sample can be used as a safe product for medical purposes and clothing applications.

Materials And Experimental Procedures

Materials

β-CD was obtained from X'ian Hong Chang Pharmaceuticals Co. (China) and KZ was gifted from Arasto Pharmaceutical Chemicals Inc. Silver nitrate 99 %, acetic anhydride, citric acid, sodium hypophosphite (SHP), methanol, ethanol and cell culture medium were used from Merck Co. (Germany). *Aspergillus niger*-ATCC 9642, *Candida albicans-ATCC 10231, Escherichia coli-* ATCC 25922 and *Staphylococcus aureus*-ATCC 2592 were also used. Sodium dioctyl sulfosuccinate and phosphate-buffered saline were purchased from Sigma-Aldrich Co. (Germany). Nonionic surfactant was procured from a local market in Tehran, Iran. Also, the bleached cotton fabric was used with 118 $g.m^{-2}$ weight from Brojerd Textile Co, Iran.

Preparation of nanocomposites solution and indicator

β-CD/KZ was prepared according to the previous report; briefly, KZ and β-CD in a molar ratio of 1:1 were stirred in the water at 25±2 °C for 3 days in the dark and the remaining solid was separated by filter paper. The pH was approximately 7±0.5 (Hedayati et al. 2020).

In order to synthesize silver nanoparticles on the β-CD/KZ nanocomposites, silver nitrate (Ag^{+}:β-CD with molar ratios of 1:50 (2 % w/w), 1:100 (1 % w/w), 1:200 (0.5 % w/w) and 1:500 (0.2 % w/w)) was added to 100 mL β-CD/KZ solution at pH=11.5 ± 0.5 adjusted with sodium hydroxide. The solution was stirred on a magnetic stirrer and heated for 3 h keeping the temperature around 80 °C.

Also, KZ was dissolved in ethanol exactly (pH = 7±0.5) with the same portion used in β-CD/KZ without β-CD.

As previously reported, the **λmax** of KZ was obtained at 243 nm with a slope of 0.0282 and R^2 = 0.994 (Hedayati et al. 2020). The obtained **λmax** conflicted with the absorbance peaks of the other compounds; thus, it was shifted to the visible range using a saturated solution of citric acid in acetic anhydride (CAA) as an indicator. Briefly, 100 mL of acetic anhydride was added to excess solid citric acid (preparing a saturated solution) stirred for 2 h and then filtered used immediately after the preparation (Omar et al. 2006). The stock solutions of KZ were produced with different concentrations of KZ in absolute methanol (Hedayati et al. 2020). 10 mL of each solution transferred to a beaker and evaporated to dry in a Bain-Marie. Then 2.5 mL of CAA indicator was added and put in Bain-Marie for 20 min kept at room temperature (20±2 °C) to cool down and then pure ethanol added to 10 mL (Omar et al. 2006). The λmax of KZ was obtained at 535 nm with a slope of 0.3615 and R^2 = 0.9916 (Y=0.3615X-0.0056) (Fig1).

Preparation of samples

The loading of nanoparticles on the cotton fabric was carried using two diverse methods (Hedayati et al. 2020). Before loading nanocomposites on the cotton fabric, the samples were washed with 1 $g.L^{-1}$ nonionic detergent for 30 min at 50 ˚C. Then the nanocomposites were loaded on the fabric in exhaustion (treating 1 h at 80 ˚C with stirring and finally drying at 80 ˚C) and padding (immersing three times in the solution and squeezing and finally drying at 80 ˚C). Further, citric acid (10 % w/w) as a cross-linking agent and sodium hypophosphite (6 % w/w) as a catalyst were added to the nanocomposites and treated on the fabric, then squeezed followed by drying at 80 ˚C. All samples were finally cured at 140 ˚C for 4 min and then rinsed with cold water. Moreover, the blank sample without β-CD was prepared with the same amount of dissolved KZ in ethanol and then loaded on the cotton fabric.

Instruments and experimental procedures

One piece of the fabric sample cut and immersed in 10 mL pure methanol (as solvent) along with stirring to study the amount of KZ entrapped in β-CD and its release rate. At a specific time (up to 30 days), the sample removed from the solution and the solution put in the bath to completely dry. Then 2.5 mL CAA indicator added and put in the bath for 20 min allowed to cool down to ambient temperature; finally, pure ethanol added to 10 mL. The KZ content was found using the UV spectra (Optizen, Mecasys, Deajoen, Korea, 2120UV) of solutions at 535 nm and the related equation (Omar et al. 2006).

The antimicrobial properties of treated samples were measured by *Aspergillus niger* (A. niger), through *FTTS-FA-006 method* and *Candida albicans (C.albicans* ATCC *10231)* fungi *using* AATCC-100-2004 method, also Gram-negative and positive *Escherichia coli (E. coli*) and *Staphylococcus aureus* (*S. aureus*) bacteria using AATCC-100-2004 method (Ghayempour and Montazer 2017; Hedayati et al. 2020).

Antifungal activity against *A. niger* (FTTS-FA-006 method):

50 mg sodium dioctylsulfosuccinate as a wetting agent was dissolved into 1 L water (0.005 %). The spores concentration was adjusted to 10^6±2×10^5 CFU/mL in a wetting agent and thoroughly shaken. The sterilized samples in diameter of 3.8+0.5 cm were placed in solid Mineral Salt Agar medium (MSA). 1±0.1

mL of the fungal spore suspension was distributed evenly over the specimen and control by micropipette. All plates were incubated at 28±1 ℃ and humidity above 85 % for 14 days. The samples were assessed by the number of spores produced on their surfaces.

Antifungal activity against *C. albicans* (AATCC 100-2004 method):

The raw (control) and treated samples were cut circular in diameter of 4.8±0.1 cm and sterilized in an autoclave. 1.0±0.1 mL of 10^5 CFU/mL microorganisms in sabouraud dextrose broth medium taken from untreated and treated fabrics and incubated at 30 ℃ for 24 h. Then, 100 mL of normal saline was added to each jar and shaken vigorously for 1 min. 1 mL of each sample was added to the plates (in duplicate) containing 15 mL sabouraud dextrose agar and mixed gently, then incubated at 37 °C for 24 h.

Antibacterial activity against *E. coli* and *S. aureus* (AATCC 100-2004 method):

The raw and treated samples were cut circular with 4.8±0.1 cm diameter and sterilized in an autoclave. 1.0 ± 0.1 mL of 10^5 CFU/mL microorganisms in triptic soy broth medium from untreated and treated fabrics were incubated at 37 ℃ for 24 h. Then, 100 mL of neutralizing solution (normal saline) was added to each jar and shaken vigorously for 1 min. 1 mL of each sample was added to plates (in duplicate) containing 15 mL triptic soy agar medium and mixed gently. The plates were incubated at 37 °C for 24 h. Then, the numbers of *colony* forming units for untreated and treated samples (A and B) were counted on the agar plates, and the reduction percentage of microbial colonies (R) was recorded according to Equation 1 (Hedayati et al. 2020; Navik 2017; Pivec el al. 2017]:

$$\text{Microbial reduction: } R\% = \frac{A-B}{A} \times 100 \qquad (1)$$

Also, the nanocomposites durability on the cotton fabric was studied through 10, 20 and 30 washes at 60 °C for 20 min with a nonionic surfactant. These samples were considered for antifungal activities against *C. albicans* (Ghayempour and Montazer 2017; Hedayati et al. 2020).

The cytotoxicity and cytocompatibility of the products on the skin is a crucial task (Ahmed et al. 2017; Martinez-Gutierrez et al. 2010; Korrapati et al. 2016). Cell culture, cytotoxicity and metabolic activity were evaluated on the normal human skin fibroblasts by MTT assay (Hedayati et al. 2020). The fibroblasts were cultured in DMEM (1X), GlutMAXTM (GibcoTM) and 10 % fetal calf serum. In order to grow and multiply natural fibroblast cells, passage number 3 was used and added to the 96-well microplates, then incubated with 5 % CO2 at 37 °C for 48 h. The raw and treated fabrics were first cut in 1×1 $inch^2$ sterilized in an autoclave (121 °C, 15 $lb/inch^2$ for 20 min). Then 2 mL cell culture medium was soaked and incubated for 24 h at 37 °C. At that point, the culture medium of multiplied cells in a 96-well microplate was slowly drained, and the samples were replaced. Finally, the microplate was incubated at 37 °C for 24 h and examined by MTT assay with 3-(4,5-dimethylthiazol-2-yl)- 2,5-diphenyltetrazolium bromide in phosphate-buffered saline. The absorption of each well was recorded by Hiperion microplatereader (MPR4+) at 570 nm, and the data were analyzed to measure the number of living cells. This was repeated

3 times and the percentage of cell viability was obtained through the absorption ratio of treated and control samples.

The composites detailed information was determined by ^{1}H-NMR in $CDCl_3$ as a solvent for KZ and D_2O for β-CD and β-CD/KZ using Ultrashield 400, BRUKER, Germany.

The dynamic light scattering (DLS) and zeta potential were used at 25 ºC by HPPSv42, Malvern Instrument, Malvern, UK, to investigate the size and surface charge of the nanocomposites.

The Fourier transform infrared spectroscopy (FTIR- Thermo Nicolet Nuexus 870 with the range 400–4000 cm^{-1}, USA) was also used to analyze the powder and treated samples such as KZ, β–CD/KZ and β–CD/KZ/Ag. For this purpose, the fabric was quite finely chopped and mixed with KBr in a ratio of 1:100.

FE-SEM as a type of electron microscope, gives an image of the sample surface with high magnification and great resolution. The MIRA3TESCAN-XMU (3-30 kV in the low vacuum) Hitachi, S-4160 was used with resolution lower than 1 nm through a magnification of 100000X, with coverage of the outer layer of samples with Au. This is also equipped with EDS microanalysis and E-map, which allows the detection of the smallest phases, with the possibility of adjusting the pressure and high resolution with an accelerating voltage of 15 kV and beam current of 1.200 nA.

The mechanical properties of samples were measured using an Instron 5566 tensile tester according to ASTM D882-02 standard in dimensions 2.5cm×15cm at a tensile speed rate of 25 mm min^{-1}. The samples were tested with the same thickness, and the results were compared.

Due to the high importance of textile hydrophilicity for medical and clothing usages, the water absorption test was performed by dropping 3 droplets of water at a distance of 1 cm from the treated samples and measuring the water spreading time three times, reporting the average time.

Air permeability test was performed on the raw and treated fabrics using Shirley air permeability tester (SDL, Atlas, USA) based on BS 5636 (Horrocks and Anand 2000).

The statistical analysis of tensile and air permeability values of raw and treated samples was performed in seven versions with five repetitions of individually treated samples, and the mean values with standard deviations (SD) reported. One-way analysis of variance (ANOVA) was performed, and the significance of each mean value was determined (P-values<0.05) with Tukey's multiple range test using GraphPad Prism version 6.0 (GraphPad Software, La Jolla, CA).

Results And Discussion

The entrapment efficiency of KZ in β-CD

The efficiency of KZ entrapment in β-CD was considered according to the total weight of KZ and β-CD and unloaded KZ in β-CD. The amount of KZ entrapped in β–CD with a molar ratio of 1:1 along shaking

at 25±2 ˚C for 3 days was about 73.6 % due to the large molecular size of KZ and a lower rate of penetration. This is an acceptable and justified value (Hedayati et al. 2020). Here, the KZ entrapment efficiency was similarly evaluated at 65 °C±3 in 3 days. After filtering the solution and drying, the residual deposit was weighed, and the efficiency of KZ entrapment in β-CD was determined by Equation 2 (Cao et al. 2019 ; Hedayati et al. 2020):

$$EE\ (\%) = (M_t - M_u)/M_t \times 100 \qquad (2)$$

M_t and Mu are the total weight of β-CD/KZ and unloaded KZ.

The entrapment efficiency of KZ in β-CD was about 73.71 %; however, due to the very high absorption in UV–Vis because of the possible KZ degradation or other phenomena, the testing at this temperature was not carried out.

^{1}H-NMR analysis of the complex

The best method to obtain a more in-depth insight into the molecular interactions between β–CD and drugs is spectroscopic and especially NMR (Conceicao et al. 2018; Demirel et al. 2011; Varga et al. 2019; Yuan et al. 2018). In this analysis, only shifts up and downfield occurred; therefore, the upfield shift of β-CD protons and downfield shift in guest protons happened because of KZ entrapment into the β-CD cavity (Chen et al. 2016; Ventura et al. 2006; Xu et al. 2015).

This test was only performed on KZ, β-CD and β-CD/KZ powder and not on β–CD /KZ/Ag-NPs due to possible toxicity. The β-CD and KZ ^{1}H-NMR spectra in Fig2 verify the prominent peaks of KZ in the ^{1}H-NMR spectra of β-CD/KZ nanocomposites confirm the KZ entrapment. Thus, the KZ molecules are entrapped into β-CDs cave mostly from -CH_3 side due to the downfield shift of H_1 (-CH_3) from 2.15 to 2.07, $H_{11\text{-}13}$, H10-14 and upfield shift H_{28}, H_{17}, H_{24} and H_{27} benzene ring of KZ (Kundu and Roy 2017; Zoppi et al. 2019).

Dynamic light scattering (DLS)

DLS recently was used to express more details on cyclodextrins accumulation (Ishiguro et al. 2010; Sajomsang et al. 2011). The colloidal stability can also be determined by the surface charge as a very effective method via zeta potential that can only be used on the nanocomposite solutions. Table 1 demonstrates the surface charge and particle size of the synthesized nanocomposites. The hydrodynamic sizes and surface charges of KZ, β-CD and β–CD /KZ were already reported (Hedayati et al. 2020) as the bigger hydrodynamic size related to β–CD and creation of hydrogen or weak physical bonding (Attarchi et al. 2013; Hedayati et al. 2020; Myles et al. 2018).

Table 1. The surface charge and particle size of diverse nanocomposites

Solutions	Hydrodynamic size		Surface charge	
(Water)	(nm)	PDI	(mV)	Zeta Deviation
KZ in ethanol	**553.5**	0.423	**-1.34**	14.3
β-CD	**1111**	0.809	**-5.17**	6.86
β-CD/KZ	**1607**	0.760	**-9.2**	8.06
β-CD/Ag (2 %)	**272.6**	0.752	**-28**	10.7
β-CD/KZ/Ag (2 %)	**904**	0.561	**-24.1**	12.1
β-CD/KZ/Ag (1 %)	**622**	0.531	**-28.2**	7.05
β-CD/KZ/Ag (0.5 %)	**406.7**	0.431	**-27.6**	3.71
β-CD/KZ/Ag (0.2 %)	**364.1**	0.456	**-24.8**	13.8

Further, The KZ with two active chlorine groups increased the hydrodynamic diameter of particles due to the possible interactions between KZ and β-CD and hydrolysis of KZ in alkali media according to Fig3, Reaction 1 (Reichle 1970). Nevertheless, KZ in an alcoholic or alkaline environment led to different Reactions (Fig3, Reaction 1 and 2) (de Almeida et al. 2019; Reichle 1970):The high temperature initiated the bigger particles with a hydrodynamic size of about 2570 nm (PDI=1.000) and surface charge of -11.3 mV (Zeta Deviation=10.2) for β–CD /KZ nanocomposites in which KZ loaded at 65±3 °C in 3 days.

The size of Ag-NPs was larger than the β-CD cavity; therefore, Ag-NPs located on the β-CD surface interacted with β-CD rim hydroxyl groups reducing the agglomeration of the particles (Attarchi et al. 2013; Ouyang et al. 2015). Thus, the Ag-NPs in the solution caused the smaller particle size in the nanometer range.

Zeta potential, as an important indicator of the colloidal solution stability, was considered (Rajamanikandan and Ilanchelian 2018). Both KZ and β-CD have a negative surface charge in an unstable range; however, the β-CD/KZ/Ag-NPs nanocomposites indicated a more negative charge, greater stability and repulsion of the particles indicated the lower aggregation and particle size (Hedayati et al. 2020).

Synthesis of Ag-NPs in β-CD/KZ

One of the proposed methods for synthesis Ag-NPs from $AgNO_3$, is using alkaline media with heating in presence of stabilizer and reducing agent such as cellulose or β-CD (Reaction.3) (Aladpoosh et al. 2014; Prasher et al. 2018; Rajamanikandan and Ilanchelian 2018; Ouyang et al. 2015). In this research, β-CD was rolled as a stabilizer and reducing agent to synthesis Ag-NPs that is negatively charged in alkaline media changed to β-CD-O^-. Ionization of the hydroxyl groups leads to β-CD-ONa^+ in sodium hydroxide solution. Ag^+ ions can replace Na^+, producing β-CD.O-Ag. This is due to the higher electronegativity of

silver (1.93) than sodium (0.93) in an aqueous solution. Also, X-ray photoelectron spectroscopic (XPS) analysis confirmed the synthesis of Ag-NPs on β-CD (Ouyang et al. 2015).

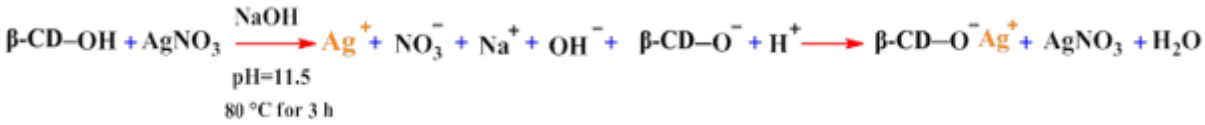

Reaction.3. Interactions of KZ, cellulose and β-CD with silver nitrate for production of AgNPs (Aladpoosh et al. 2014; Ouyang et al. 2015).

Drug release

Drug release was studied based on the amount of drug-loaded on the cotton fabric repeated for three times. A color indicator was used to measure the amount of KZ. Similar percentages of KZ release were already reported for samples treated with KZ and β–CD /KZ in ethanol for both methods using the standard curve (Hedayati et al. 2020). However, in order to reduce the possible errors, no color indicator was used for nanoparticle-free solutions. The highest percentage and amount of KZ loaded on the fabric related to the exhaustion method. Also, the release behavior of KZ from different samples with or without β-CD was thoroughly discussed (Hedayati et al. 2020). Here, the effect of Ag-NPs on release of KZ was investigated. According to Table 2 and Fig4.a, synthesis of Ag-NPs in the solution containing β-CD/KZ led to the lower loading of nanocomposites or KZ release from the fabric in both practical methods. This can be related to the decrease in aggregation due to the silver NPs (Attarchi et al. 2013; Ouyang et al. 2015).

For those samples with Ag-NPs, the test was performed on β-CD/KZ/Ag 2 % in two methods.

Table 2. KZ content of different treated cotton fabrics

Samples	Method	Weight (mg)	KZ (mg)	KZ (%)
KZ	Exhaustion	160	0.073	0.045
β-CD/KZ	Exhaustion	140	0.354	0.253
β-CD/KZ	Padding	166	0.119	0.072
β-CD/KZ/Ag 2%	Exhaustion	150	0.190	0.127
β-CD/KZ/Ag 2%	Padding	158	0.080	0.051

Fig4-b shows the slower, regular and more linear KZ release rate for the samples containing Ag-NPs even after 30 days, and a partial release of KZ observes after 40 days. The hydrophobic internal cavity of β-CD is about 0.78 nm, allowing very small synthesized silver NPs to enter the cavity without the silver nucleation. The Ag ions can react with hydroxyl groups of β-CD and hydrolyzed parts of KZ in an alcoholic or alkaline environment. This proportionate to the state of KZ entry into the β-CD cavity as the

KZ molecule entrapped into β-CD cave mostly from -CH3 side according to the ^{1}H-NMR spectra. Hence, the rate of KZ release can be slowed down by increasing the size of composites. Moreover, the nucleation mostly formed on the hydroxyl groups of the β-CD oriented out of the structure and Ag-NPs are likely acting to block the route for releasing KZ from the β-CD cavity (Fig3). This can be considered a reason for the slow release of KZ from those samples having Ag-NPs (Jaiswal et al. 2010).

Generally, KZ and β-CD/KZ loaded on the cotton fabric have a very slow release rate because of the unique structure of KZ with two active chlorine groups. These can react with hydroxyl groups of β-CD or cellulose fibers to create a covalent bond between KZ and cellulose (Hedayati et al. 2020). Also, the synthesis of Ag-NPs in an alkaline environment led to KZ hydrolysis, and its reaction with Ag or β-CD hydroxyl groups caused the prolonged release of KZ (Hedayati et al. 2020; Lewis 2011]. The negative charge on KZ makes ready for the placement of Ag^{+} (Fig3, Reaction 2) (de Almeida et al. 2019).

Antimicrobial activity of treated samples

Two fungus and yeasts, *A. niger* and *C. albicans* and two Gram negative and positive bacteria, *E. coli* and *S. aureus* were selected to study the antimicrobial activities of the treated samples (Table 3).

Table 3. Antimicrobial activities of different treated samples

Samples	Method	*C. albicans*				*A. niger*	*E. coli*	*S. aureus*
			Washing stability (%)					
			10 run	10 run	10 run			
Blank		**0**	0	0	0	**0**	**0**	**0**
KZ	Exhaustion	**100**	100	99.5	99	**90**	**0**	**2**
β-CD/KZ	Exhaustion	**100**	100	100	100	**81**	**0**	**1**
β-CD/KZ	Padding	**96**	80	73	60	**50**	**0**	**0**
β-CD/Ag: 2%	Exhaustion	**70**	70	68	65	**42**	**84**	**80**
β-CD/KZ/Ag : 2%	Padding	**100**	97	95	93	**71**	**55**	**51**
β-CD/KZ/Ag : 2%	Exhaustion	**100**	100	100	100	**98**	**87**	**83**
β-CD/KZ/Ag 1%	Exhaustion	**100**	—	—	—	**96.7**	**70**	**63**
β-CD/KZ/Ag : 0.5%	Exhaustion	**100**	—	—	—	**95**	**50**	**50**
β-CD/KZ/Ag : 0.2%	Exhaustion	**100**	—	—	—	**91.3**	—	—

The antimicrobial activities of KZ and β-CD/KZ and the loading method effects have already been reported. As such, the antifungal activities of exhausted samples are much stronger than padded ones because of the high temperature, fibers swelling, greater pore size and more loading of nanocomposites in the exhaustion method (Hedayati et al. 2020). However, none of those prepared samples with KZ showed antibacterial activity. Ag-NPs are sticking to microorganism membranes disrupting the function and making holes in the membrane and cytoplasmic fluid outflow, causing cell death (Vale et al. 2019; Wenhao et al. 2020). Hence, Ag-NPs were synthesized on the β-CD/KZ composites to investigate their effects on the padded and exhausted samples. β-CD/Ag 2% showed 70, 42, 87 and 82 % microbial reduction for *C. albicans*, *A. niger*, *E. coli* and *S. aureus*, respectively. All samples containing KZ were affected on *C. albicans*; however, the Ag-NPs indicated potential effects on *A. niger*. Among various samples, β-CD/KZ/Ag 2 % indicated the best antifungal and antibacterial effects. Although the amount of KZ in β-CD/KZ was much more than β-CD/KZ/Ag in the exhaustion method, a weaker fungicidal effect was observed on *A. niger*. Based on the above results, Ag-NPs and KZ with great improved effects can advance the final antimicrobial properties (Falahati et al. 2014).

Washing durability

The washing durability of samples was examined against *C. albicans* and the percentages of growth inhibition are reported in Table 3. The good washing durability has already been shown on the treated samples with KZ and β-CD/KZ via exhaustion method (Hedayati et al. 2020). The effect of Ag-NPs on the nanocomposites after various washes exhibited very high washing durability; however, the exhausted samples revealed better durability than padded ones. This can be due to the processing at high-temperature along with mechanical movements that led to the fibers swelling, pores formation, and greater loading of the nanocomposites onto the fibers. These caused covalent bonds between the nanocomposites and the cellulosic chains of fabric.

The sample loaded with β-CD/Ag exhibited good washing durability after 30 washes as the antifungal properties decreased from 70 to 65 %, possibly due to Ag cations reaction or cationic charged Ag-NPs with hydroxyl groups of β-CD and cotton (Fig3).

Cell culture and cytotoxicity

The used dosage of KZ and β-CD indicated no cytotoxic effects on the human fibroblasts skin (Hedayati et al. 2020). The cytotoxicity of Ag-NPs in different concentrations was examined due to its importance for wound dressings and underwear. All treated samples illustrated no cytotoxic effects on the human fibroblasts confirming safety of the products for skin (Fig 5). This confirmed no side effects on the human skin with loading of a very low Ag-NPs on the samples.

Fourier transform infrared spectroscopy (FTIR)

FTIR spectra explore the chemical structure of materials and nanocomposites loaded on the fabrics. The exhausted samples were selected to be analyzed due to the more loading of nanocomposites with the

highest Ag-NPs on the cotton fabric. Fig 6 displays the FTIR spectrum of pure KZ powder, raw and treated fabrics with nanocomposites. The prominent peaks of KZ, cotton and cross-linked β-CD on fabric (at 1726 cm^{-1}) were thoroughly discussed previously (Hedayati et al. 2020).

The increase in the absorbance intensity of prominent KZ peaks, such as C-N stretching or C=C aromatic rings on the treated samples, confirmed KZ entrapment or loading on the fabric. However, the lack of KZ prominent peak at 814 cm^{-1} related to C–Cl stretching on the treated fabric proved the removal of chlorine groups due to the chlorine reacts with the hydroxyl groups of cotton fabric (Hedayati et al. 2020).

The peak at 3334 cm^{-1} (O-H stretching) confirmed Ag-NPs and the shift of peak to 3345 cm^{-1} with lower intensity could be related to the synthesis of Ag-NPs within the β-CD/KZ structure. There are no significant changes in other prominent peaks of cotton, such as 1006 and 1032 (C–O stretching), 1112 (C–O–C glucose ring) and 2901 cm^{-1} (C–H stretching).

Field Emission Scanning Electron Microscopy (FE-SEM), Elemental mapping (E-map) and EDS spectrum

The FE-SEM, EDS and E-map pictures of raw and exhausted samples with the most properties are displayed in Fig 7 indicated the surface topography and identified the elements and uniformity of their distribution.

The image of raw cotton fabric with the fibrils on the surface can be realized in Fig7; however, the treated fabric with nanocomposites entirely covered with the nanocomposites. The aggregation of particles can be seen in some parts, especially on β-CD/KZ due to the high β-CD content creating hydrogen, covalent or van der Waals bonds between β-CDs or β-CD/KZ. However, Ag-NPs potentially reduced the aggregation of the nanocomposites.

The particle size of KZ and β-CD/KZ is about 40-65 nm, while 20-40 nm for β-CD/KZ/Ag. The E-map also confirmed the uniformity of KZ and Ag-NPs on all samples. The amounts of Cl and N groups can be specified to KZ in the following order: β-CD/KZ > β-CD/KZ/Ag > KZ

Energy-dispersive X-ray spectroscopy (EDS) was used to identify elements, including Ag (Urban et al. 2009) (Fig7). The peaks of carbon and oxygen are associated with KZ and cellulose structure of cotton and β-CD. The loading of β-CD on fabric led to the strong peaks of carbon and oxygen elements. The small peaks of chlorine and nitrogen corresponding to KZ can be observed. A very low intensity of chlorine peak compared with nitrogen indicated a possible reaction of chlorine with hydroxyl groups of β-CD or cotton fabric. The Au is also associated with a gold layer for preparing the sample.

Tensile properties

The tensile strength of raw and treated cotton samples with nanocomposites is revealed in Table 4, screening the effects of nanocomposites and citric acid on the cotton fabric. Based on the previous study, the more loading of nanocomposites on the cotton fabric (without fixation) caused a significant (P-values<0.05) increase in the fabric strength due to the bonds created with the cellulosic chains of cotton

fabric. It is claimed that the reaction of KZ with cotton fabric led to higher tensile strength. Also, the β-CD/KZ with citric acid on cotton fabric caused the lower tensile strength due to the acid degradation of cellulosic chains at high temperatures. This can be partially improved with increasing β-CD in the exhaustion method (P-values<0.05) (Hedayati et al. 2020).

It is certain that the treated fabric with β-CD (P-values<0.05) has higher tensile strength (225.6 N) than β-CD/KZ (219.38 N) because of the entrapped KZ into β-CD cavity or bonding with its rim hydroxyl groups and lower β-CD loading. The Ag-NPs somehow reduced β-CD gathering and nanocomposites content on the cotton fabric, consequently reduced the tensile strength (196.07 N) (P-values<0.05). In general, the tensile strength of samples is within the acceptable range. An ANOVA analysis indicated that the amount of nanocomposites loaded on the fabric fixed with citric acid significantly affected the tensile strength ($p<0.05$).

Water absorption

The water absorption test was performed, and the average of three repeated tests are reported in Table 4. The β-CD, KZ and Ag-NPs on the surface of cotton fibers improved the water absorption. The rate of spreading and absorption of water droplets on all samples was fast, close to zero second time.

Air permeability

Air permeability test was performed on the raw and treated fabric samples at a test pressure drop of 50 Pa for 5 cm^2 test area. This was repeated three times, and the averages are reported in Table 4. The nanocomposites treated sample airflow rates are almost similar and somehow more than the raw sample due to reducing the lateral fibers and increasing the pore size for air to pass through the fabric. On the other hand, the application of nanocomposites on cotton fabric at high temperature somehow increased the fabric air permeability (P-values<0.05).

Table 4. Other physical properties of the treat samples

Samples	Method	Tensile		Water absorption	Air permeability	
		(N)	CV%	Absorption time (s)	($mL.s^{-1}cm^{-2}$)	CV%
Blank	----------	247.35	0.3	0	150	0.2
KZ	Exhaustion	261.54	0.5	0	190	0.2
β-CD	Exhaustion	225.6	0.7	0	180	0.3
β-CD/KZ	Exhaustion	219.38	1.1	0	180	0.5
β-CD/KZ	Padding	185.69	1.2	0	178	0.4
β-CD/Ag 2%	Exhaustion	206.1	1.6	0	160	0.7
β-CD/KZ/Ag 2%	Exhaustion	196.07	1.5	0	155	0.8
β-CD/KZ/Ag 2%	Padding	177.73	1.3	0	185	0.7
β-CD/KZ/Ag 1%	Exhaustion	-------	---	---	---	---
β-CD/KZ/Ag0.5%	Exhaustion	-------	---	---	---	---
β-CD/KZ/Ag0.2%	Exhaustion	-------	---	---	---	---

Conclusion

In this study, β-CD/KZ/Ag nanocomposites were produced and applied on the cotton fabric via two diverse methods of exhaustion and padding created a novel antimicrobial drug delivery system. The final products were characterized by using various analyzing tools. The exhaustion method is mostly recommending due to the much more nanocomposites loading on cotton fabric than padding. The best antimicrobial effects reported on the sample treated with β-CD/KZ/Ag 2 % indicating 100 % reduction of *C. albicans* and *A. niger* fungi and about 85 % reduction of *E. coli* and *S. aureus* with no cytotoxic effects. The Ag-NPs in the composites prevented the nanoparticle aggregation lowered the nanocomposites content on the cotton fabric, possibly reducing the drug side effects. The placements of Ag-NPs within and around β-CD/KZ nanocomposites may cause the closure of β-CD cavity and reduce the KZ release with more regularity. Finally, the good durability of β-CD/KZ/Ag nanocomposites on the cotton fabric in consecutive washes leads to the superior antimicrobial activities, breathability, water and moisture absorption with reasonable tensile strength that can be offered as a good product to be used as the antifungal and antibacterial substrate.

Declarations

No funds, grants, or other support was received.

The authors have no conflicts of interest to declare that are relevant to the content of this article.

References

Abarca, R. L., Rodriguez, F. J., Guarda, A., Galotto, M. J., & Bruna, J. E. (2016). Characterization of beta-cyclodextrin inclusion complexes containing an essential oil component. *Food Chemistry*, *196*, 968-975. https://doi.org/10.1016/j.foodchem.2015.10.023

Ahmed, K. B. R., Nagy, A. M., Brown, R. P., Zhang, Q., Malghan, S. G., & Goering, P. L. (2017). Silver nanoparticles: Significance of physicochemical properties and assay interference on the interpretation of in vitro cytotoxicity studies. *Toxicology in Vitro*, *38*, 179-192. https://doi.org/10.1016/j.tiv.2016.10.012

Aladpoosh, R., Montazer, M., & Samadi, N. (2014). In situ green synthesis of silver nanoparticles on cotton fabric using Seidlitzia rosmarinus ashes. *Cellulose*, *21*(5), 3755-3766. https://doi.org/10.1007/s10570-014-0369-1

Attarchi, N., Montazer, M., & Toliyat, T. (2013). Ag/TiO_2/β-CD nano composite: preparation and photo catalytic properties for methylene blue degradation. *Applied Catalysis A: General*, *467*, 107-116. https://doi.org/10.1016/j.apcata.2013.07.018

Benita, S. (2006). *Microencapsulation methods and industrial applications* (2nd edition).USA: CRC Press.

Cao, F., Rodriguez-Hornedo, N., & Amidon, G. E. (2019). Mechanistic analysis of cocrystal dissolution, surface pH, and dissolution advantage as a guide for rational selection. *Journal of Pharmaceutical Sciences*, *108*(1), 243-251. https://doi.org/10.1016/j.xphs.2018.09.028

Che, J., Wu, Z., Shao, W., Guo, P., Lin, Y., Pan, W. & Xu, Y. (2015). Synergetic skin targeting effect of hydroxypropyl-β-cyclodextrin combined with microemulsion for ketoconazole. *European Journal of Pharmaceutics and Biopharmaceutics*, *93*, 136-148. https://doi.org/10.1016/j.ejpb.2015.03.028

Chen, X., Qiu, Y. K., Owh, C., Loh, X. J., & Wu, Y. L. (2016). Supramolecular cyclodextrin nanocarriers for chemo-and gene therapy towards the effective treatment of drug resistant cancers. *Nanoscale*, *8*(45), 18876-18881. https://doi.org/10.1039/C6NR08055C

Conceicao, J., Adeoye, O., Cabral-Marques, H. M., & Lobo, J. (2018). Cyclodextrins as drug carriers in pharmaceutical technology: the state of the art. *Current Pharmaceutical Design*, *24*(13), 1405-1433. https://doi.org/10.2174/1381612824666171218125431

de Almeida, R. F., Santos, F. C., Marycz, K., Alicka, M., Krasowska, A., Suchodolski, J., ... & Starosta, R. (2019). New diphenylphosphane derivatives of ketoconazole are promising antifungal agents. *Scientific reports, 9*(1), 1-14. https://doi.org/10.1038/s41598-019-52525-7

Demirel, M., Yurtdaş, G., & Genç, L. (2011). Inclusion complexes of ketoconazole with beta-cyclodextrin: physicochemical characterization and in vitro dissolution behaviour of its vaginal suppositories. *Journal*

of Inclusion Phenomena and Macrocyclic Chemistry, *70*(3-4), 437-445. https://doi.org/10.1007/s10847-010-9922-1

Durán, N., Durán, M., De Jesus, M. B., Seabra, A. B., Fávaro, W. J., & Nakazato, G. (2016). Silver nanoparticles: A new view on mechanistic aspects on antimicrobial activity. *Nanomedicine: Nanotechnology, Biology and Medicine*, *12*(3), 789-799.https://doi.org/10.1016/j.nano.2015.11.016

Falahati, M., Nozari, S., Makhdoomi, A., Ghasemi, Z., Nami, S., & Assadi, M. (2014). Comparison of antifungal effect of nanosilver particles alone and in combination with current drugs on Candida species isolated from women with recurrent vulvovaginal candidiasis. *Eur J Exp Biol*, *4*(1), 77-82.

Farokhi, M., Mottaghitalab, F., Fatahi, Y., Khademhosseini, A., & Kaplan, D. L. (2018). Overview of silk fibroin use in wound dressings. *Trends in Biotechnology*, *36*(9), 907-922. https://doi.org/10.1016/j.tibtech.2018.04.004

Ghayempour, S., & Montazer, M. (2017). Ultrasound irradiation based in-situ synthesis of star-like Tragacanth gum/zinc oxide nanoparticles on cotton fabric. *Ultrasonics Sonochemistry*, *34*, 458-465. https://doi.org/10.1016/j.ultsonch.2016.06.019

Gupta, A., Briffa, S. M., Swingler, S., Gibson, H., Kannappan, V., Adamus, G. & Radecka, I. (2020). Synthesis of silver nanoparticles using curcumin-cyclodextrins loaded into bacterial cellulose-based hydrogels for wound dressing applications. *Biomacromolecules*. Published online. https://doi.org/10.1021/acs.biomac.9b01724

Hedayati, N., Montazer, M., Mahmoudirad, M., & Toliyat, T. (2020). Ketoconazole and Ketoconazole/β-cyclodextrin performance on cotton wound dressing as fungal skin treatment. *Carbohydrate Polymers*, 116267. https://doi.org/10.1016/j.carbpol.2020.116267

Horrocks, A. R., & Anand, S. C. (Eds.). (2000). *Handbook of Technical Textiles*. Elsevier.

Ishiguro, T., Hirayama, F., Iohara, D., Arima, H., & Uekama, K. (2010). Crystallization and polymorphic transitions of chlorpropamide in aqueous 2-hydroxybutyl-β-cyclodextrin solution. *European Journal of Pharmaceutical Sciences*, *39*(4), 248-255. https://doi.org/10.1016/j.ejps.2009.12.008

Jaiswal, S., Duffy, B., Jaiswal, A. K., Stobie, N., & McHale, P. (2010). Enhancement of the antibacterial properties of silver nanoparticles using β-cyclodextrin as a capping agent. *International Journal of Antimicrobial Agents*, *36*(3), 280-283. https://doi.org/10.1016/j.ijantimicag.2010.05.006

Jiang, X., Fan, X., Xu, W., Zhang, R., & Wu, G. (2019). Biosynthesis of Bimetallic Au-Ag Nanoparticles Using Escherichia coli and its Biomedical Applications. *ACS Biomaterials Science & Engineering*, *6*(1), 680-689. https://doi.org/10.1021/acsbiomaterials.9b01297

Kaur, I. P., & Kakkar, S. (2010). Topical delivery of antifungal agents. *Expert Opinion on Drug Delivery*, *7*(11), 1303-1327. https://doi.org/10.1517/17425247.2010.525230

Kaushik, C. P., Pahwa, A., Thakur, R., & Kaur, P. (2017). Regioselective synthesis and antimicrobial evaluation of some thioether–amide linked 1, 4-disubstituted 1, 2, 3-triazoles. *Synthetic Communications*, *47*(4), 368-378.https://doi.org/10.1080/00397911.2016.1265983

Kim, H. S., Sun, X., Lee, J. H., Kim, H. W., Fu, X., & Leong, K. W. (2019). Advanced drug delivery systems and artificial skin grafts for skin wound healing. *Advanced Drug Delivery Reviews*, *146*, 209-239. https://doi.org/10.1016/j.addr.2018.12.014

Korrapati, P. S., Karthikeyan, K., Satish, A., Krishnaswamy, V. R., Venugopal, J. R., & Ramakrishna, S. (2016). Recent advancements in nanotechnological strategies in selection, design and delivery of biomolecules for skin regeneration. *Materials Science and Engineering: C*, *67*, 747-765. https://doi.org/10.1016/j.msec.2016.05.074

Kundu, M., & Roy, M. N. (2017). Preparation, interaction and spectroscopic characterization of inclusion complex of a cyclic oligosaccharide with an antidepressant drug. *Journal of Inclusion Phenomena and Macrocyclic Chemistry*, *89*(1-2), 177-187. https://doi.org/10.1007/s10847-017-0745-1

Lee, E. J., Huh, B. K., Kim, S. N., Lee, J. Y., Park, C. G., Mikos, A. G., & Choy, Y. B. (2017). Application of materials as medical devices with localized drug delivery capabilities for enhanced wound repair. *Progress in Materials Science*, *89*, 392-410. https://doi.org/10.1016/j.pmatsci.2017.06.003

Lewis, D. M. (2011). The chemistry of reactive dyes and their application processes. In *Handbook of textile and industrial dyeing* (pp. 303-364). Woodhead Publishing. https://doi.org/10.1533/9780857093974.2.301

Martinez-Gutierrez, F., Olive, P. L., Banuelos, A., Orrantia, E., Nino, N., Sanchez, E. M., ... & Av-Gay, Y. (2010). Synthesis, characterization, and evaluation of antimicrobial and cytotoxic effect of silver and titanium nanoparticles. *Nanomedicine: Nanotechnology, Biology and Medicine*, *6*(5), 681-688. https://doi.org/10.1016/j.nano.2010.02.001

Myles, A., Behan, J. A., Twamley, B., Colavita, P. E., & Scanlan, E. M. (2018). Spontaneous Aryldiazonium grafting for the preparation of functional cyclodextrin-modified materials. *ACS Applied Bio Materials*, *1*(3), 825-832. https://doi.org/10.1021/acsabm.8b00266

Navik, R., Thirugnanasampanthan, L., Venkatesan, H., Kamruzzaman, M., Shafiq, F., & Cai, Y. (2017). Synthesis and application of magnesium peroxide on cotton fabric for antibacterial properties. *Cellulose*, *24*(8), 3573-3587. https://doi.org/10.1007/s10570-017-1356-0

Ning, Y., Shen, W., & Ao, F. (2020). Application of blocking and immobilization of electrospun fiber in the biomedical field. *RSC Advances*, *10*(61), 37246-37265. https://doi.org/10.1039/D0RA06865A

Omar, M. A., Abuo-Rahma, G. E. D. A., & Abdelmageed, O. H. (2006). Colorimetric determination of certain antifungals in pure forms and in their pharmaceutical formulations. *Bulletin of Pharmaceutical Sciences.*

Assiut, *29*(2), 501-519. https://doi.org/10.21608/BFSA.2006.65229

Ouyang, L., Zhu, L., Ruan, Y., & Tang, H. (2015). Preparation of a native β-cyclodextrin modified plasmonic hydrogel substrate and its use as a surface-enhanced Raman scattering scaffold for antibiotics identification. *Journal of Materials Chemistry C*, *3*(29), 7575-7582. https://doi.org/10.1039/C5TC01368B

Pinho, E., Henriques, M., & Soares, G. (2014). Cyclodextrin/cellulose hydrogel with gallic acid to prevent wound infection. *Cellulose*, *21*(6), 4519-4530. https://doi.org/10.1007/s10570-014-0439-4

Pivec, T., Hribernik, S., Kolar, M., & Kleinschek, K. S. (2017). Environmentally friendly procedure for in-situ coating of regenerated cellulose fibres with silver nanoparticles. *Carbohydrate polymers*, *163*, 92-100. https://doi.org/10.1016/j.carbpol.2017.01.060

Prasher, P., Singh, M., & Mudila, H. (2018). Silver nanoparticles as antimicrobial therapeutics: current perspectives and future challenges. *3 Biotech, 8*(10), 411. https://doi.org/10.1007/s13205-018-1436-3

Radu, C. D., Parteni, O., & Ochiuz, L. (2016). Applications of cyclodextrins in medical textiles. *Journal of Controlled Release*, *224*, 146-157. https://doi.org/10.1016/j.jconrel.2015.12.046

Rajamanikandan, R., & Ilanchelian, M. (2018). Naked eye and optical biosensing of cysteine over the other amino acids using β-cyclodextrin decorated silver nanoparticles as a nanoprobe. *New Journal of Chemistry*, *42*(11), 9193-9199. https://doi.org/10.1039/C7NJ05164F

Rameshkumar, N., Ashokkumar, M., Subramanian, E. H., Ilavarasan, R., & Sridhar, S. K. (2003). Synthesis of 6-fluoro-1, 4-dihydro-4-oxo-quinoline-3-carboxylic acid derivatives as potential antimicrobial agents. *European Journal of Medicinal Chemistry*, *38*(11-12), 1001-1004. https://doi.org/10.1016/S0223-5234(03)00151-X

Rana, M., Hao, B., Mu, L., Chen, L., & Ma, P. C. (2016). Development of multi-functional cotton fabrics with Ag/AgBr–TiO_2 nanocomposite coating. *Composites Science and Technology*, *122*, 104-112. https://doi.org/10.1016/j.compscitech.2015.11.016

Reichle, W. T. (1970). The nature of the hydrolysis of chlorobenzene over calcium phosphate apatite. *Journal of Catalysis*, *17*(3), 297-305.https://doi.org/10.1016/0021-9517(70)90104-1

Sajomsang, W., Gonil, P., Ruktanonchai, U. R., Pimpha, N., Sramala, I., Nuchuchua, O., ... & Puttipipatkhachorn, S. (2011). Self-aggregates formation and mucoadhesive property of water-soluble β-cyclodextrin grafted with chitosan. *International journal of biological macromolecules*, *48*(4), 589-595. https://doi.org/10.1016/j.ijbiomac.2011.01.028

Sedighi, A., Montazer, M., & Hemmatinejad, N. (2014). Copper nanoparticles on bleached cotton fabric: in situ synthesis and characterization. *Cellulose*, *21*(3), 2119-2132. https://doi.org/10.1007/s10570-014-0215-5.

Sharaf, S., & El-Naggar, M. E. (2019). Wound dressing properties of cationized cotton fabric treated with carrageenan/cyclodextrin hydrogel loaded with honey bee propolis extract. *International journal of biological macromolecules*, *133*, 583-591. https://doi.org/10.1016/j.ijbiomac.2019.04.065

Urban, V. M., Seó, R. S., Giannini, M., & Arrais, C. A. G. (2009). Superficial distribution and identification of antifungal/antimicrobial agents on a modified tissue conditioner by SEM-EDS microanalysis: a preliminary study. *Journal of Prosthodontics: Implant, Esthetic and Reconstructive Dentistry*, *18*(7), 603-610. https://doi.org/10.1111/j.1532-849X.2009.00479.x

Vale, A. C., Pereira, P., Barbosa, A. M., Torrado, E., Mano, J. F., & Alves, N. M. (2019). Antibacterial free-standing polysaccharide composite films inspired by the sea. *International journal of biological macromolecules*, *133*, 933-944. https://doi.org/10.1016/j.ijbiomac.2019.04.102

Varga, E., Benkovics, G., Darcsi, A., Várnai, B., Sohajda, T., Malanga, M., & Béni, S. (2019). Comparative analysis of the full set of methylated β-cyclodextrins as chiral selectors in capillary electrophoresis. *Electrophoresis*, *40*(21), 2789-2798. https://doi.org/10.1002/elps.201900134

Veerakumar, P., Sangili, A., Chen, S. M., & Lin, K. C. (2020). Ultrafine gold nanoparticle embedded poly (diallyldimethylammonium chloride)–graphene oxide hydrogels for voltammetric determination of an antimicrobial drug (metronidazole). *Journal of Materials Chemistry C, 8,* 7575-7590. https://doi.org/10.1039/C9TC06690J

Ventura, C. A., Giannone, I., Musumeci, T., Pignatello, R., Ragni, L., Landolfi, C. & Puglisi, G. (2006). Physico-chemical characterization of disoxaril–dimethyl-β-cyclodextrin inclusion complex and in vitro permeation studies. *European Journal of Medicinal Chemistry*, *41*(2), 233-240. https://doi.org/10.1016/j.ejmech.2005.11.002

Wang, Y., Kaur, G., Chen, Y., Santos, A., Losic, D., & Evdokiou, A. (2015). Bioinert anodic alumina nanotubes for targeting of endoplasmic reticulum stress and autophagic signaling: a combinatorial nanotube-based drug delivery system for enhancing cancer therapy. *ACS Applied Materials & Interfaces*, *7*(49), 27140-27151. https://doi.org/10.1021/acsami.5b07557

Wenhao, Z., Zhang, T., Yan, J., Li, Q., Xiong, P., Li, Y., ... & Zheng, Y. (2020). In vitro and in vivo evaluation of structurally-controlled silk fibroin coatings for orthopedic infection and in-situ osteogenesis. *Acta Biomaterialia, 116*, 223-245. https://doi.org/10.1016/j.actbio.2020.08.040

Wu, T., Lu, F., Wen, Q., Yu, K., Lu, B., Rong, B., ... & Lan, G. (2018). Novel strategy for obtaining uniformly dispersed silver nanoparticles on soluble cotton wound dressing through carboxymethylation and in-situ reduction: antimicrobial activity and histological assessment in animal model. *Cellulose*, *25*(9), 5361-5376. https://doi.org/10.1007/s10570-018-1907-z

Xu, L., Zhang, W., Cai, H., Liu, F., Wang, Y., Gao, Y., & Zhang, W. (2015). Photocontrollable release and enhancement of photodynamic therapy based on host–guest supramolecular amphiphiles. *Journal of*

Materials Chemistry B, *3*(37), 7417-7426. https://doi.org/10.1039/C5TB01363A

Yao, X., Huang, P., & Nie, Z. (2019). Cyclodextrin-based polymer materials: from controlled synthesis to applications. *Progress in Polymer Science*, *93*, 1-35. https://doi.org/10.1016/j.progpolymsci.2019.03.004

Yuan, Y., Zhang, Q., Yan, Y., Gong, M., Zhao, Q., Bao, Z. & Wang, S. (2018). Designed construction of tween 60@ 2β-CD self-assembly vesicles as drug delivery carrier for cancer chemotherapy. *Drug Delivery*, *25*(1), 623-631. https://doi.org/10.1080/10717544.2018.1440448

Zoppi, A., Buhlman, N., Cerutti, J. P., Longhi, M. R., & Aiassa, V. (2019). Influence of proline and β-Cyclodextrin in ketoconazole physicochemical and microbiological performance. *Journal of Molecular Structure*, *1176*, 470-477. https://doi.org/10.1016/j.molstruc.2018.08.094

Figures

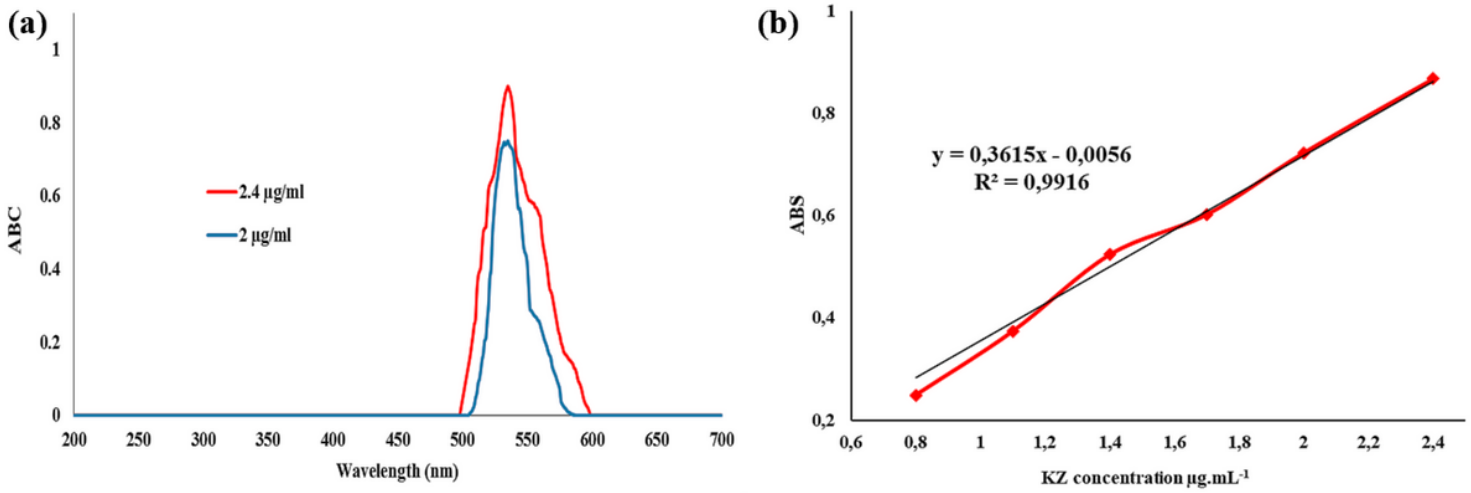

Figure 1

(a)UV/Vis absorbance spectra of KZ dissolved in methanol at 2 and 2.4 µg.mL-1 (b). KZ calibration curve at λ=535 nm

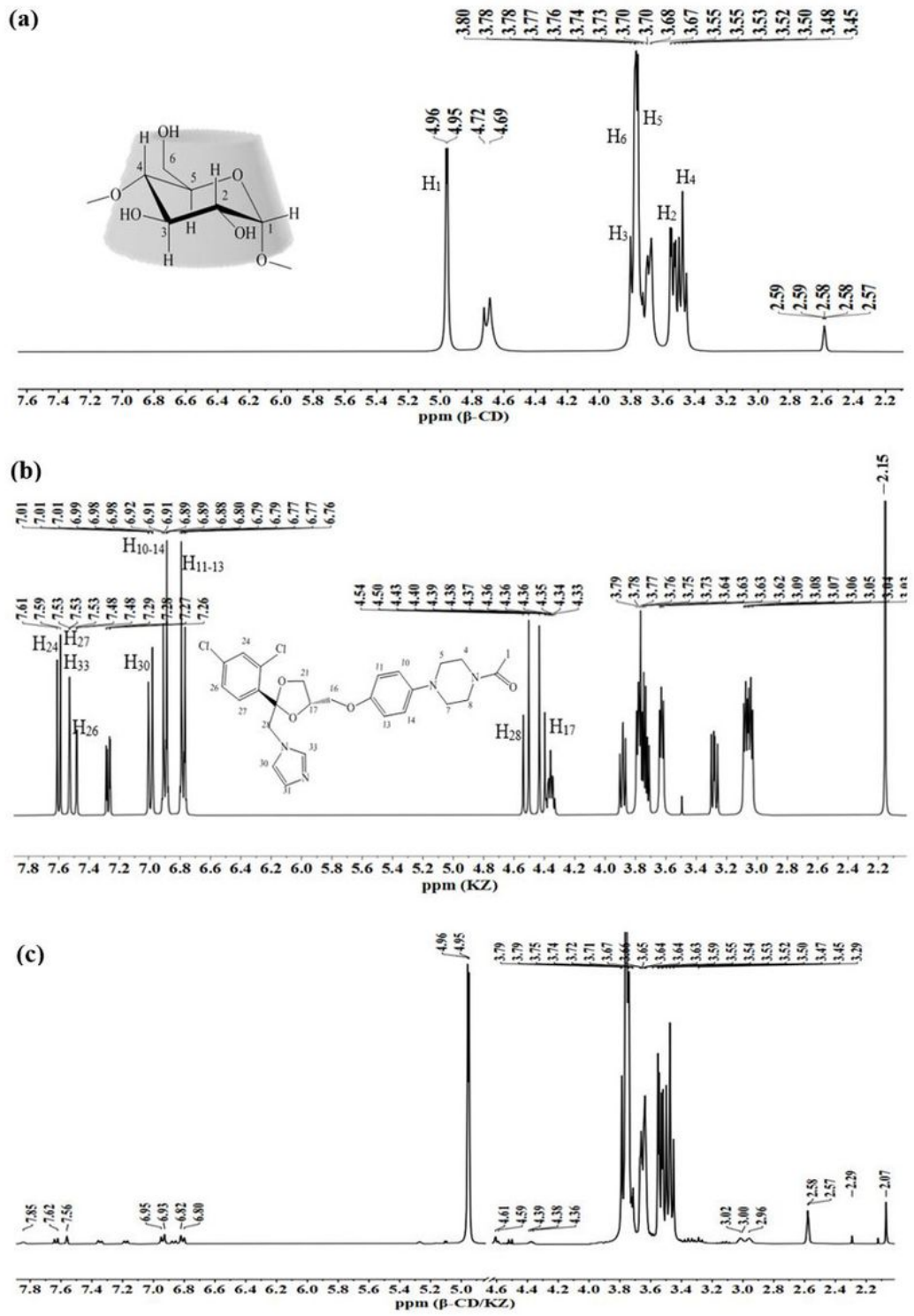

Figure 2

1H-NMR spectra of pure (a) KZ, (b) pure β-CD and (c) β-CD/KZ composites

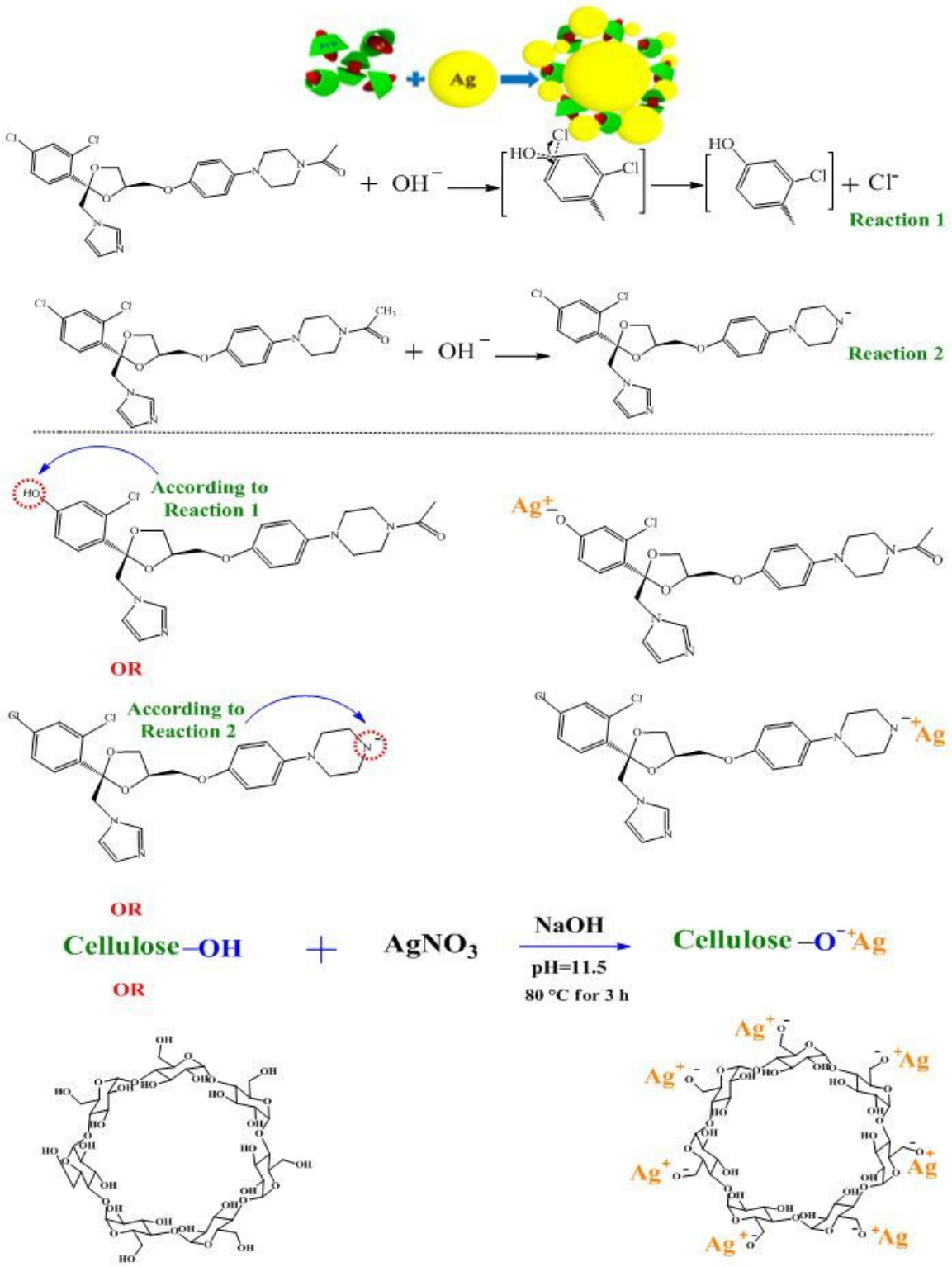

Figure 3

Reaction 1: Possible hydrolysis of KZ in the dichlorophenyl side (Reichle 1970) Reaction 2: Possible hydrolysis of KZ in the ethanone side (de Almeida et al. 2019) and Interactions of KZ, cellulose and β-CD with silver nitrate for production of Ag-NPs (Attarchi et al. 2013; de Almeida et al. 2019; Prasher et al. 2018; Rameshkumar et al. 2003).

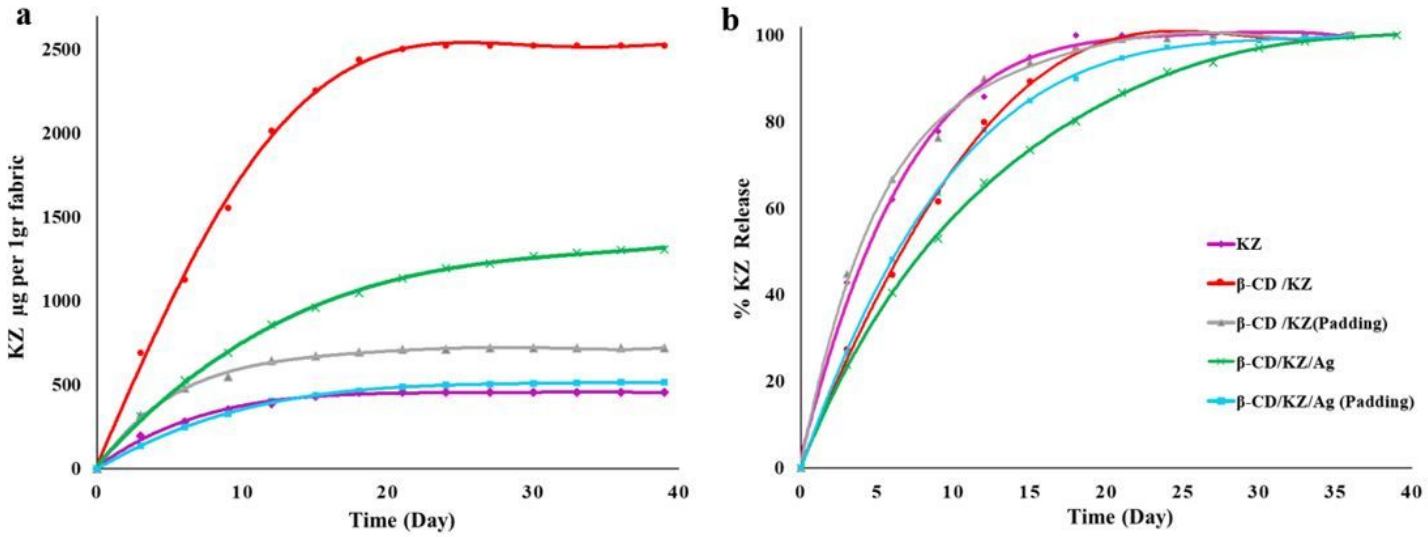

Figure 4

The release rate of KZ from different treated samples in methanol containing the color indicator

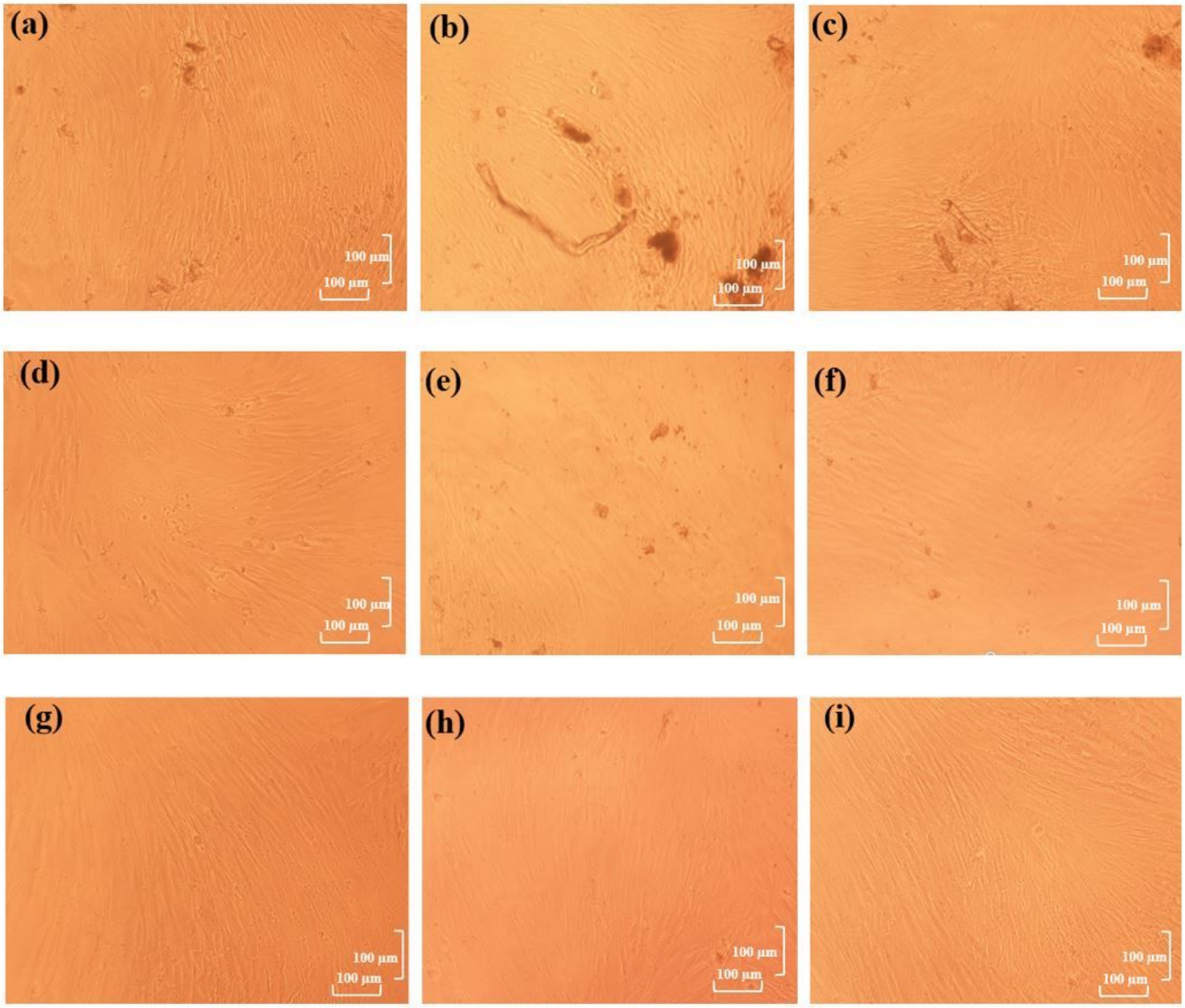

Figure 5

Cell growth images of various treated cotton samples (a) KZ, (b) β-CD/KZ, (c) β-CD/KZ padded (d) β-CD/Ag 2 %, (e) β-CD/KZ/Ag 2 %, (f) β-CD/KZ/Ag 2 % padded, (g) β-CD/KZ/Ag 1 %, (h) β-CD/KZ/Ag 0.5 %, (i) β-CD/KZ/Ag 0.2 %.

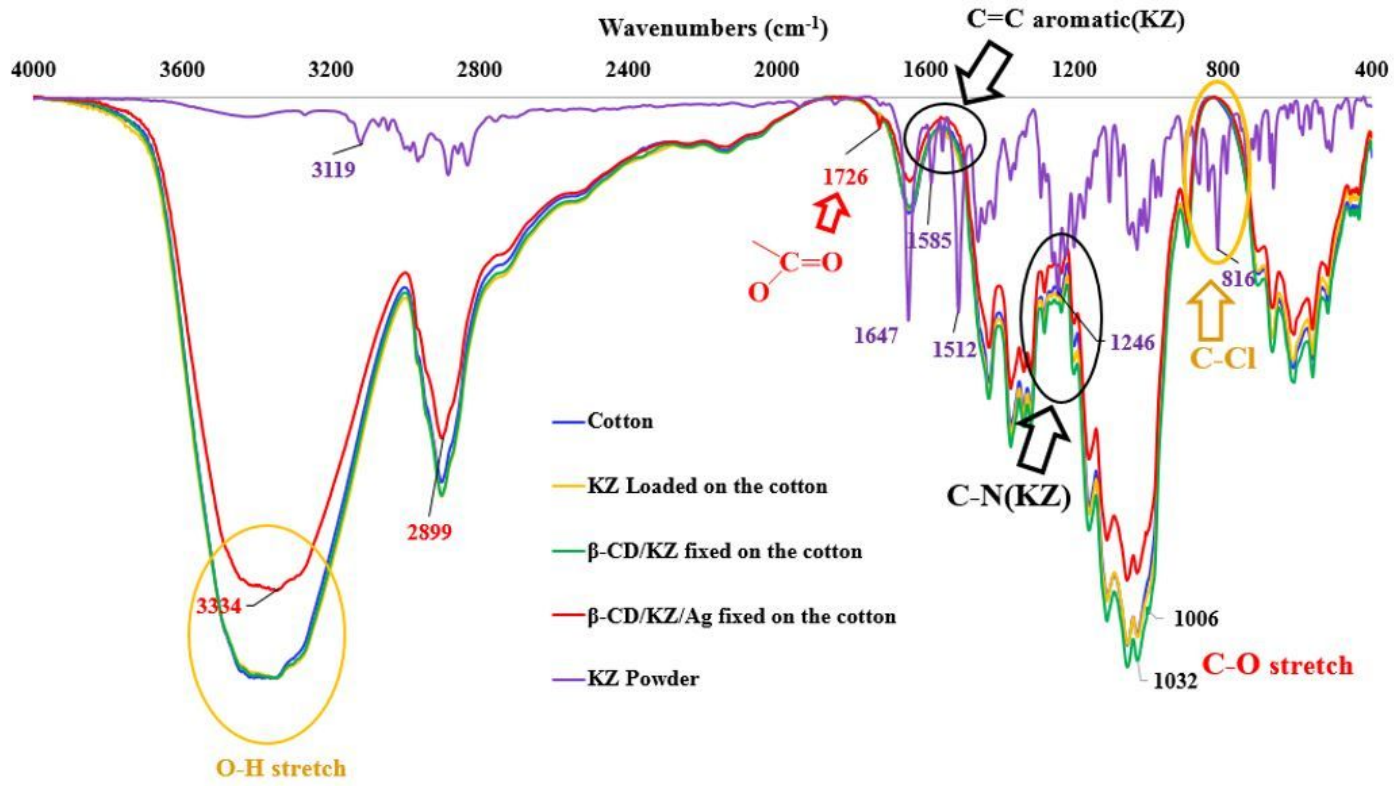

Figure 6

FTIR spectra of pure KZ powder, raw and treated cotton fabrics with diverse nanocomposites.

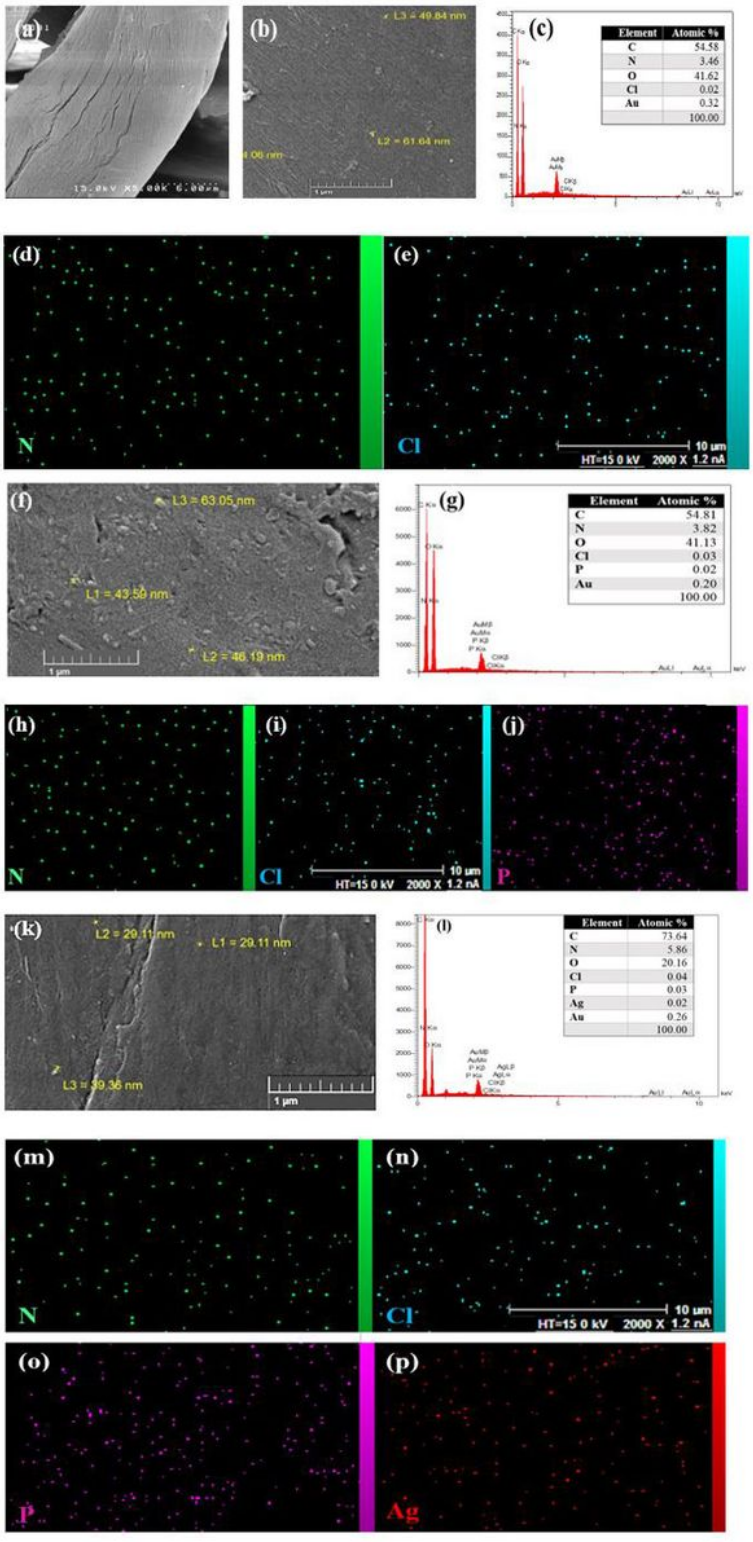

Figure 7

FE-SEM, EDS and E-map images of different cotton samples (a) blank, (b-e) treated with KZ, (f-j) treated with β-CD/KZ, (k-p) treated with β-CD/KZ/Ag 2%